PHYSICAL REVIEW B **73**, 224407 (2006)

Double stripe ordering in $Nd_{0.5}Sr_{0.5}MnO_3$ determined by resonant soft x-ray scattering

Javier Herrero-Martín,[1] Joaquín García,[1] Gloria Subías,[1] Javier Blasco,[1] María Concepción Sánchez,[1] and Stefan Stanescu[2]
[1]*Instituto de Ciencia de Materiales de Aragón, Departamento de Física de la Materia Condensada, CSIC-Universidad de Zaragoza, Pedro Cerbuna 12, 50009 Zaragoza, Spain*
[2]*European Synchrotron Radiation Facility, Boîte Postal 220, F-38043 Grenoble Cedex, France*
(Received 2 March 2006; published 6 June 2006)

We have studied the low-temperature ordered phase of $Nd_{0.5}Sr_{0.5}MnO_3$ by resonant soft x-ray scattering at the Mn $L_{2,3}$ edges. Strong resonances were observed at $(0\ \frac{1}{2}\ 0)$ and $(\frac{1}{2}\ 0\ 0)$ reflections, which are resolved in momentum space. Azimuthal scans reveal a π periodicity for both resonances, the minimum intensity being almost zero. The two reflections show a very different energy dependence which extends in the whole energy region of the Mn L-edge. The $(0\ \frac{1}{2}\ 0)$ reflection originates from the anisotropy induced on the d-symmetry projected density of states owing to the local tetragonal distortion at one of the two crystallographic inequivalent Mn sites (the so-called Mn^{3+} ions in the conventional ionic description). This is similar to the resonance observed at the Mn K edge. We propose that the $(\frac{1}{2}\ 0\ 0)$ reflection, which has not its counterpart either on the Mn K-edge resonant scattering or on the magnetic scattering, is originated by anisotropy of the d-symmetry projected density of the so-called Mn^{4+} sublattice. In this way, the latter reflection could denote a pure orbital ordering in this sublattice.

DOI: 10.1103/PhysRevB.73.224407 PACS number(s): 75.47.Lx, 78.70.Ck, 71.30.+h

I. INTRODUCTION

During the last years the interest focused on mixed valence manganese oxides of the type $RE_{1-x}A_xMnO_3$, $RE_{1-x}A_{1+x}MnO_4$ and $RE_{2-2x}A_{1+2x}Mn_2O_7$ (*RE*: rare earth, *A*: alkaline earth) has grown due to the recent discovery of magnetoresistance.[1–3] This feature was the outbreak to highlight the strong interplay between charge, and orbital and magnetic properties exhibited by these compounds. Accordingly, they show a wide variety of electronic and magnetic phases.[2–4]

Near the half-doping composition, the formal valence of Mn atoms is 3.5+ and most of the studied manganites undergo a structural transition at the so-called charge ordering temperature T_{CO}, accompanied by the appearance of a charge and orbital modulation,[5–10] the so-called charge and orbital ordering (CO and OO). This is reflected in the observance of electronic and magnetic superstructures by means of resonant x-ray scattering (RXS). RXS is the most suitable technique[11] for unraveling the CO and OO nowadays because of the combined element and site selectivity it provides. The most commonly accepted arrangement for the low-temperature ordered phase in half-doped manganites is the checkerboard pattern.[8,12] Manganese atoms are surrounded octahedrally by oxygen anions. There are two kinds of Mn environments: Mn forming nearly regular MnO_6 (hereafter denoted as "even-Mn") and Mn in tetragonally distorted MnO_6 (denoted as "odd-Mn"). They alternate in the unit cell following a zigzag chain as indicated in Fig. 1. The structural anisotropy direction of two consecutive "odd-Mn" is approximately 45° tilted with respect to the a and b axes of the cell and forming a 90° angle with respect to each other. This structural distortion causes a redistribution of the charge density between the two kinds of Mn atoms. Some authors

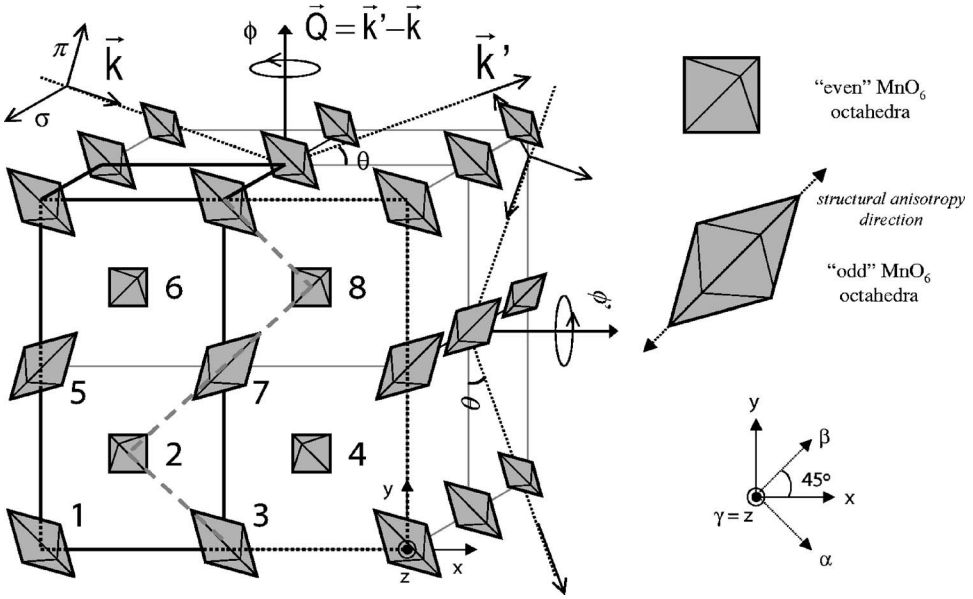

FIG. 1. Crystallographic structure of the $Nd_{0.5}Sr_{0.5}MnO_3$ and experimental diffraction configuration for measuring the $(0\ \frac{1}{2}\ 0)$ and $(\frac{1}{2}\ 0\ 0)$ resonant reflections. Dashed lines indicate the zig-zag FM chains. The $\{x,y,z\}$ and $\{\alpha,\beta,\gamma\}$ coordinates reference frames are also depicted. The $\boldsymbol{\sigma}$ polarization of the incident beam is perpendicular to the a axis for ϕ=90°.

have described these phases below T_{CO} in terms of ionic CO: the "even-Mn" and "odd-Mn," are associated with Mn^{4+} and Mn^{3+} ions, respectively.[13–17] A RXS study at the Mn *K* edge of $Nd_{0.5}Sr_{0.5}MnO_3$ has shown that the charge segregation is much less than 1 electron, $Mn^{3.4+}$ and $Mn^{3.6+}$ for odd and even Mn, respectively.[18] This result seems to be reproduced in other half-doped manganites.[19–21]

Simultaneous to the appearance of superlattice reflections associated to a charge modulation between both kinds of Mn atoms, forbidden reflections have also been observed in RXS experiments at the Mn *K* edge[13–18,22] due to the anisotropy of the atomic scattering tensor (so-called anisotropic tensor susceptibility or ATS reflections) The structure factor of those ATS reflections is given by the difference between odd-Mn atoms with different orientation of their anisotropy axis in the *ab* plane (Fig. 1). The intensity of these diffraction peaks has been proven to have the same azimuthal periodicity as the "so-called CO" reflections show.[18] The ATS (so-called OO) reflections tested at the Mn *K* edge reflect the differences on the *p*-symmetry projected density of empty states at the Mn site. It has been claimed that this anisotropy in the Mn *p* band arises from the hybridization between 3*d* and Mn 4*p* states through O 2*p* ones. Accordingly, the appearance of ATS reflections at the Mn *K* edge has been proposed as a probe of OO. In contrast, several authors have shown that the sensitivity of the resonant scattering at the Mn *K* edge to orbital modulation mainly lies on Jahn-Teller distortions and band structure effects rather than on 3*d*-4*p* Coulomb interaction.[23,24]

However, it has not been until very recently that technological developments have brought to the scientific community the availability to carry out RXS experiments in the region of soft x-rays (resonant soft x-ray scattering, RSXS). RSXS experiments at the Mn $L_{2,3}$ edges measure the transition probability from 2*p* to *d*-symmetry Mn projected states and give out an accurate measurement of the distribution of the *d*-electronic density in the empty Mn band. We would like to clarify here that x-ray absorption (or x-ray anomalous scattering) measures the density of empty states of a given symmetry projected on the resonant site. In this sense, RSXS gives information on anisotropy of the *d*-component of the extended orbitals at the transition metal site but it cannot be considered as a measure of different orbital occupation. In the ionic approximation, i.e., the orbitals are localized at the atoms, the interpretation of the RSXS experiments in terms of OO is completely justified. However, this approach is quite rough and could give rise to an overinterpretation of the RSXS results as a direct probe of OO.[25] For the sake of comparison with previous surveys, we will maintain the term OO in the sense of *d* anisotropy of the local electronic density of empty states. Furthermore, RSXS has also been used to study the magnetic structure in these materials.

Several RSXS works at Mn $L_{2,3}$ edges have been recently published for half-doped manganites with unit cells of different dimensionality like $La_{0.5}Sr_{1.5}MnO_4$,[21,26–28] $LaSr_2Mn_2O_7$,[29,30] and $Pr_{0.6}Ca_{0.4}MnO_3$.[19,20] In most of these works, the tetragonal symmetry does not allow us to distinguish between the (100) and (010) domains. As a consequence, the analysis of the origin of the reported RSXS turns out to be very complicated. A fundamental advantage of the present work with respect to the preceding experiments is that we have studied a $Nd_{0.5}Sr_{0.5}MnO_3$ single crystal where the orthorhombic unit cell allows us to separately analyze the $(\frac{1}{2}\ 0\ 0)$ and $(0\ \frac{1}{2}\ 0)$ reflections. As we will show later, strong resonances are observed at the Mn $L_{3,2}$ absorption edge for both reflections. Since the $(\frac{1}{2}\ 0\ 0)$ reflection cannot be originated either from the tetragonal distortion or from the magnetic order,[31] we propose that this reflection has its origin on the *d* asymmetry of the even-Mn sublattice.

II. EXPERIMENTAL

The single crystal of $Nd_{0.5}Sr_{0.5}MnO_3$ was grown at the Zaragoza University using a floating zone furnace. The structure corresponds to an orthorhombic distorted perovskite with lattice constants $a=5.515$ Å, $b=5.452$ Å, and $c=7.552$ Å at $T=60$ K (*Ibmm* setting). The crystal resulted to be twinned along the (100)/(010) directions. The crystal was cut and polished in a plane defined by these vectors.

We measured the $(0\ \frac{1}{2}\ 0)$ and $(\frac{1}{2}\ 0\ 0)$ reflections at the energy of the Mn $L_{2,3}$ absorption edge by means of RXS. The experiment was performed at the beam line ID08 of the ESRF in Grenoble, France. In this beamline, two Apple II undulators provide a high flux of 100% circular or linear (π and σ) polarized light tunable in the energy range from 400 to 1500 eV with an energy resolution of 0.2 eV at 650 eV. The beam is monochromatized by a spherical grating monochromator having a total flux of about 10^{12} photons/s on the sample. The sample was mounted with silver paint on a 3+2-circle UHV diffractometer provided with a refrigerator system (cold finger and copper braids) giving access to a temperature range at the sample stage from 20 K up to 300 K, which allows the goniometer to be rotated around the scattering vector to perform azimuthal scans.

In half-doped manganites of the type $RE_{1-x}A_xMnO_3$, $(0\ k/2\ 0)$ *k* odd reflections have been described as originating from the ordering of the 3*d* orbitals of the "Mn^{3+}" atoms (odd Mn in Fig. 1). Measurements were taken at different azimuthal angles, varying from 0° up to 90°, and at several temperatures ranging from 30 K to 180 K. Both $(0\ \frac{1}{2}\ 0)$ and $(\frac{1}{2}\ 0\ 0)$ reflections are present with a nearly constant intensity at low temperatures up to $T_{CO} \sim T_N \sim 160$ K, and they disappear around 180 K.

III. RESULTS

Figure 2 shows the energy dependence of the $(0\ \frac{1}{2}\ 0)$ reflection for σ linear polarization of the incident beam in the vicinity of the Mn L_3 ($2p_{3/2} \rightarrow 3d$) and L_2 ($2p_{1/2} \rightarrow 3d$) absorption edges. The absorption spectrum is also shown for the sake of comparison. The energy scan of Fig. 2 displays clear features at both edges. Two main peaks appear at the L_3 edge and two other peaks are observed at the L_2 edge. The first and most intense resonant peak (labeled *A*) appears at the L_3 edge. It is located at 641.7 eV while the second and weaker peak (labeled *B*) appears 2.3 eV beyond. The other couple of peaks appear within the L_2 region at 652.2 eV (peak *C*) and 653.8 eV (peak *D*). There are also two broad features, denoted as S1 and S2, at 648 and 658 eV, i.e., about

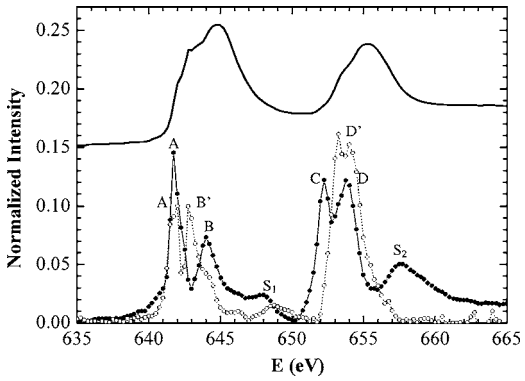

FIG. 2. Top: absorption spectrum measured at the Mn $L_{2,3}$ edges in total electron yield configuration at 200 K (thick solid line). Bottom: normalized intensity of the $(\frac{1}{2}\ 0\ 0)$ (solid line+open circles) and $(0\ \frac{1}{2}\ 0)$ (solid line+closed circles) reflections are shown as a function of the incident energy at 30 K and $\phi=90°$ for σ linear polarization of the incident beam. Main features in the spectra have been labeled. The energy scan of $(\frac{1}{2}\ 0\ 0)$ has been normalized multiplying by 3.

4 eV beyond the second peak of each couple of peaks.

The comparison to previous measurements in related compounds such as $La_{0.5}Sr_{1.5}MnO_4$ (Refs. 21 and 26–28, $Pr_{0.6}Ca_{0.4}MnO_3$ (Ref. 19), or $LaSr_2Mn_2O_7$ (Refs. 29 and 30) reveals that the scattered intensity always shows the presence of these two couples of peaks together with two broad features (see Fig. 3). However, the relative intensity of these resonances seems to be different for each compound. Surprisingly, the resonant spectral shapes of the $(0\ \frac{1}{2}\ 0)$ reflection in $Nd_{0.5}Sr_{0.5}MnO_3$ and the so-called OO resonance published for $LaSr_2Mn_2O_7$ at 20 K (Ref. 29) are nearly identical as shown in Fig. 3.

The dependence of the integrated intensity of this reflection at 641.7 eV (peak *A* in Fig. 2) with the azimuthal angle ϕ yields a π periodicity with a maximum for $\phi=\pi/2$ (see Fig. 4), in agreement with our previous results reported at the Mn *K* edge[18] for the equivalent $(0\ \frac{5}{2}\ 0)$ reflection. We have checked that the energy dependence of the scattered intensity

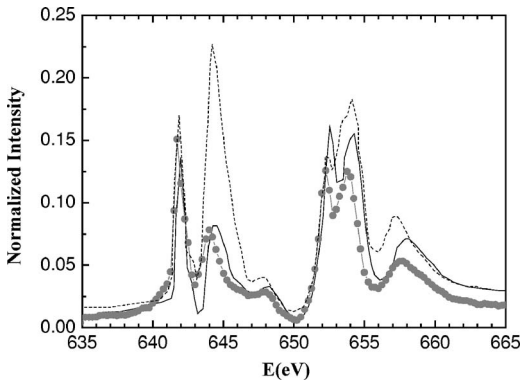

FIG. 3. Normalized intensity of the $(0\ \frac{1}{2}\ 0)$ reflection as a function of the incident photon energy in $Nd_{0.5}Sr_{0.5}MnO_3$ (filled circles) at 30 K compared to the energy scans reported for $LaSr_2Mn_2O_7$ at 20 K, by Wilkins *et al.*[29] (solid line) and for $La_{0.5}Sr_{1.5}MnO_4$ at 40 K by Staub *et al.*[28] (dotted line).

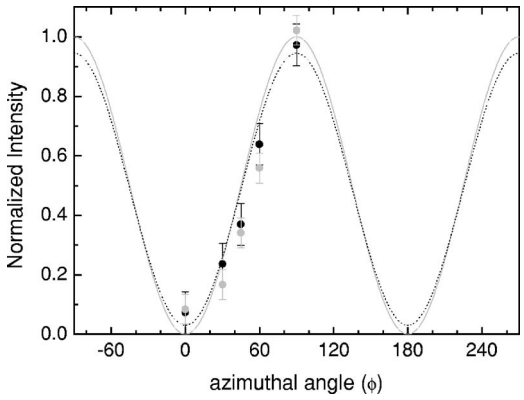

FIG. 4. Normalized integrated intensity of the peak *A* feature at 641.7 eV for both $(0\ \frac{1}{2}\ 0)$ and $(\frac{1}{2}\ 0\ 0)$ reflections, indicated by filled gray and black circles, respectively, for different values of the azimuthal angle ϕ. Solid and dotted lines are simulations of the expected azimuthal dependence for the intensity of the $(0\ \frac{1}{2}\ 0)$ and $(\frac{1}{2}\ 0\ 0)$ reflections with incident σ polarization, respectively.

is independent of the azimuthal angle chosen. This azimuthal behavior is characteristic of a dipolar E1 resonant scattering process and it concurs with the dependence observed in other manganites.

Figure 2 also shows the energy dependence for the intensity of the $(\frac{1}{2}\ 0\ 0)$ reflection at the Mn $L_{2,3}$ edges with σ polarization of the incident beam. The average intensity of this reflection is about three times lower than that of the $(0\ \frac{1}{2}\ 0)$ reflection. The energy scan also reveals the presence of a couple of peaks for each edge, but in this case there is a higher overlapping between them. Two peaks are observed (A' and B') at the L_3 edge, which are separated by roughly 1 eV. The separation is even less for the couple of peaks at the L_2 edge, giving rise to a broader resonance centered at ~653.5 eV (D'). The A' feature appears at the same energy as peak *A* in the $(0\ \frac{1}{2}\ 0)$ reflection, but the B' feature is shifted to lower energies in comparison to peak *B*. Moreover, the broad feature S2 is lacking for this reflection. Finally, the strongest resonances are now located at the L_2 edge. These differences for the energy line shape between both reflections support the idea that these signals originated from different sublattices. In particular, it is noteworthy that the L_3/L_2 intensity ratios of the resonances are approximately $\frac{2}{3}$ and 1 for $(\frac{1}{2}\ 0\ 0)$ and $(0\ \frac{1}{2}\ 0)$ reflections, respectively.

The azimuthal dependence for the integrated intensity of the $(\frac{1}{2}\ 0\ 0)$ reflection is similar to that observed for $(0\ \frac{1}{2}\ 0)$, as shown in Fig. 4. It follows a sine wave of π period with similar maxima and minima. The energy line shape is also independent of the azimuthal angle for this reflection.

We have also studied the temperature evolution of the resonant intensity for both reflections upon warming through $T_{CO}\approx T_N\approx 160$ K.[31] The results are plotted in Fig. 5. It can be seen that the intensity of both reflections monotonically decays on heating disappearing at around 180 K. However, no change in the line shape is observed (Fig. 5).

Figure 6 shows the temperature evolution of selected features indicated in Fig. 2. This evolution clearly demonstrates that resonant scatterings at both reflections arise from the

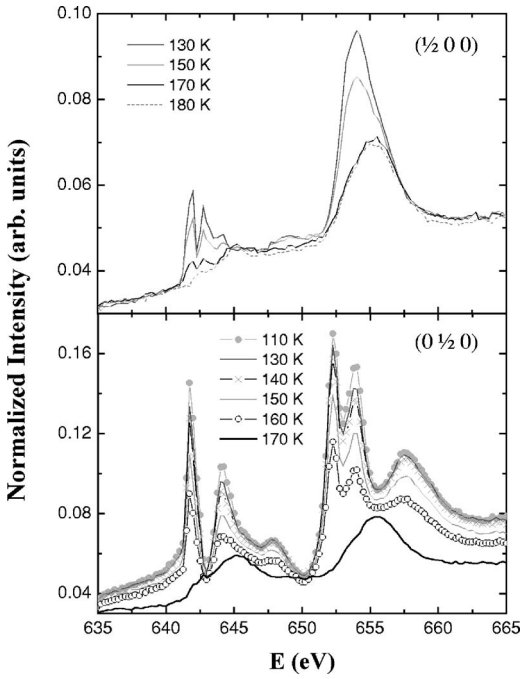

FIG. 5. Raw energy scans of $\left(\frac{1}{2}\ 0\ 0\right)$ (top) and $\left(0\ \frac{1}{2}\ 0\right)$ (bottom) resonant reflections without fluorescence background subtraction as a function of temperature across $T_{CO} \cong T_N$.

structural and magnetic transitions that take place around 160 K. However, small differences are observed in their thermal evolutions. Resonances seem to appear at slightly higher temperature for the $\left(\frac{1}{2}\ 0\ 0\right)$ reflection than for the $\left(0\ \frac{1}{2}\ 0\right)$ one.

IV. DISCUSSION

It is well known that $Nd_{0.5}Sr_{0.5}MnO_3$ undergoes a structural transition at T_{CO}, giving rise to two inequivalent crystallographic sites for the Mn atoms in the low-temperature cell, the odd- and even-Mn (Fig. 1). In a previous work,[18] we have studied the so-called OO reflection $\left(0\ \frac{5}{2}\ 0\right)$ by using RXS measurements at the Mn *K* edge. We demonstrated a structural origin for the $(0\ k/2\ 0)$ reflections owing to the different orientation of the anisotropy axis in the odd-Mn atoms following a zig-zag chain in the *ab* plane (Fig. 1), i.e., these OO reflections are in fact ATS reflections. In this framework, the atomic scattering factors should be described by using a tensorial formalism.[32–34] It is worth pointing out that similar azimuthal behavior can be obtained from the atomic approach given by Hannon *et al.*,[35] but the tensorial analysis is more general and appropriate.

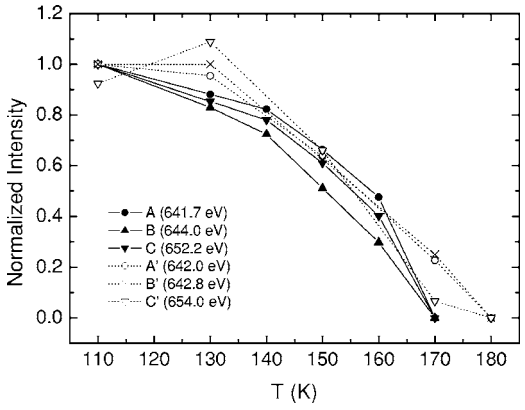

FIG. 6. Temperature dependence of the intensity of the main features shown in the energy scans of Fig. 2 for the $\left(0\ \frac{1}{2}\ 0\right)$ (closed symbols) and $\left(\frac{1}{2}\ 0\ 0\right)$ reflections (open symbols). Solid and dashed lines are merely a guide to the eye and the intensities have been normalized at 100 K.

Therefore, in the present study of the $\left(0\ \frac{1}{2}\ 0\right)$ and $\left(\frac{1}{2}\ 0\ 0\right)$ reflections at the Mn $L_{3,2}$ edge, we use the same tensorial analysis performed in the RXS study at the Mn *K* edge. We have chosen a reference frame $\{\alpha, \beta, \gamma\}$, where the unit vectors follow the direction of the Mn-O bonds in the distorted octahedra (Fig. 1). In the dipolar approximation, this makes the anomalous scattering factor of the odd-Mn atoms be a diagonal tensor of rank 2. Following Fig. 1, the even-Mn atoms can be considered as regular octahedron (the anomalous scattering factor is scalar), whereas for the odd-Mn atoms the elongated Mn-O bonds are oriented along the α direction in sites 1 and 3 whereas they follow the β direction in sites 5 and 7. In a first approximation, the four short Mn-O bonds can be considered as identical and the three elements in the diagonal can be approximated by only two different components: one for the direction of the structural anisotropy, denoted as parallel ($\parallel$), and the other one perpendicular ($\perp$), along the two perpendicular directions of the short Mn-O bonds. Thus,

$$f_5 = f_7 = \begin{pmatrix} f_\perp & 0 & 0 \\ 0 & f_\parallel & 0 \\ 0 & 0 & f_\perp \end{pmatrix}; \quad f_1 = f_3 = \begin{pmatrix} f_\parallel & 0 & 0 \\ 0 & f_\perp & 0 \\ 0 & 0 & f_\perp \end{pmatrix}. \quad (1)$$

We now transform these f_i tensors into the reference frame of the crystal $\{x, y, z\}$ (Fig. 1). The new f_i^* tensors turn out to be

$$f_5^* = f_7^* = \begin{pmatrix} \frac{f_\perp + f_\parallel}{2} & \frac{-f_\perp + f_\parallel}{2} & 0 \\ \frac{-f_\perp + f_\parallel}{2} & \frac{f_\perp + f_\parallel}{2} & 0 \\ 0 & 0 & f_\perp \end{pmatrix},$$

$$f_1^* = f_3^* = \begin{pmatrix} \frac{f_\perp + f_\parallel}{2} & \frac{f_\perp - f_\parallel}{2} & 0 \\ \frac{f_\perp - f_\parallel}{2} & \frac{f_\perp + f_\parallel}{2} & 0 \\ 0 & 0 & f_\perp \end{pmatrix}. \quad (2)$$

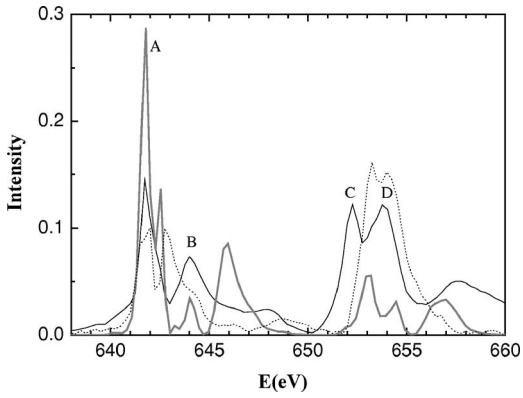

FIG. 7. Comparison between the $(0\ \frac{1}{2}\ 0)$ and $(\frac{1}{2}\ 0\ 0)$ resonant reflections (solid and dotted black lines, respectively) with σ incident radiation and the square of the derivative of the absorption spectrum at the Mn $L_{2,3}$ edges (thick gray line).

In the unit cell described in Fig. 1, the structure factors F of the two studied reflections (note that the even atoms do not give any contribution) can be written as

$$F\left(0\tfrac{1}{2}0\right) = f_5^* + f_7^* - f_1^* - f_3^* = 2\begin{pmatrix} 0 & (f_\parallel - f_\perp) & 0 \\ (f_\parallel - f_\perp) & 0 & 0 \\ 0 & 0 & 0 \end{pmatrix},$$

$$F\left(\tfrac{1}{2}00\right) = f_5^* - f_7^* + f_1^* - f_3^* = 0. \quad (3)$$

The scattering intensity will depend on the polarization of both the incident and scattered light, the polarization dependence being the same as that previously reported at the Mn K edge.[18] It is then straightforward to deduce that $I_{\sigma\sigma'}(0\ \frac{1}{2}\ 0) = I_{\pi\pi'}(0\ \frac{1}{2}\ 0) = 0$. On the other hand, the scattered intensity for $\sigma \rightarrow \pi'$ and $\pi \rightarrow \sigma'$ channels yields

$$I_{\sigma\pi'}\left(0\tfrac{1}{2}0\right) = I_{\pi\sigma'}\left(0\tfrac{1}{2}0\right) = 4(f_\parallel - f_\perp)^2 \cos^2\theta \sin^2\phi, \quad (4)$$

where 2θ is the scattering angle and ϕ is the azimuthal angle around the scattering vector. This means that the same dependence on the energy, polarization and azimuthal rotation of the scattered intensity must be observed no matter whether the incident radiation is σ or π polarized.

No polarization analysis was performed and thus we directly measured the total scattered intensity. The comparison of a simulation of the azimuthal dependence given by Eq. (4) to the experimental $(0\ \frac{1}{2}\ 0)$ intensity shows a fair qualitative agreement, as seen in Fig. 4.

The energy dependence of the scattered intensity probes the anisotropy in the Mn-projected empty density of states with d symmetry. Within the tensorial model, only two components ($f_\parallel$ and $f_\perp$) of the atomic scattering tensor are needed to describe these forbidden reflections. At the K edge, the anisotropy can be well described by means of an anisotropic energy shift between the two components. Instead, the situation in the $L_{2,3}$ edge is more complicated. A simulation assuming a rigid energy shift between $f_\parallel$ and $f_\perp$ components does not reproduce the experimental data. Moreover, the anisotropy is reflected in the whole energy range of the L_3/L_2 absorption spectrum. For the sake of illustration, Fig. 7 shows the comparison between the resonant spectrum and the square of the derivative of the absorption spectrum which can be considered as a first approximation as an energy shift. Several attempts[25,36] have been made to reproduce the experimental RXS spectrum at the $L_{2,3}$ edge in other half-doped manganites, but all of them use the atomic multiplet approach from a perfect ionic ordering, i.e., the anisotropy comes from the ordering of $3d$ orbitals of Mn^{3+} ions. However, we have shown in our Mn K edge study that the charge segregation is too small for considering the approach of an integer valence at the Mn atoms as valid. Nevertheless, we will try to obtain some qualitative conclusions from Fig. 7. We observe that the first peak at L_3 (A) and L_2 (C) edges can be ascribed to a derivative effect originated by a shift of the first empty d state on the basis of the atomic picture, reflecting the anisotropy of this particular d state symmetry. On the other hand, the second peaks at L_3 (B) and L_2 (D) edges would indicate the presence of anisotropy associated with other d states of different symmetries. In other words, the d anisotropy extends to the whole p-d Mn band, making it very difficult to conciliate it with an atomic OO description. Moreover, different resonances are observed at the L_3 and L_2 edges, which indicates that the spin-orbit coupling must be taken into account to describe the RXS spectra.

We can conclude that the $(0\ \frac{1}{2}\ 0)$ resonance has the same origin as the equivalent resonance at the Mn K edge. The local structural distortion induces anisotropy on the projection at the Mn sites of the electronic band structure; on the p symmetry at the K edge and on the d-symmetry projection at the $L_{2,3}$ edges.

Regarding the $(\frac{1}{2}\ 0\ 0)$, no intensity was observed either in the $\sigma \rightarrow \sigma'$ or $\sigma \rightarrow \pi'$ channels at the Mn K edge.[18] No contribution is expected from the anisotropy of the odd-Mn sublattice, as deduced from Eq. (3). Moreover, this resonant reflection cannot be ascribed to the AFM ordering developed below $T_N \approx T_{CO} \approx 160$ K because such magnetic reflection was not observed in its neutron diffraction pattern.[31] We note that the CE-type spin ordering implies that ab planes stack antiferromagnetically along the c axis. The magnetic reflections for both odd-Mn and even-Mn sublattices are then limited to the Miller index l=odd integer.

The azimuthal dependence of $(\frac{1}{2}\ 0\ 0)$ is similar to the $(0\ \frac{1}{2}\ 0)$ reflection (Fig. 4), suggesting that an equivalent tensorial analysis would describe this azimuthal behavior. The main differences between both reflections corresponds to their energy line shape. The simultaneous observation of these two reflections seems to be contradictory because they show two different oriented stripes. On one hand, the $(\frac{1}{2}\ 0\ 0)$ reflection indicates a stripe order on the (1 0 0) direction and, on the other hand, the $(0\ \frac{1}{2}\ 0)$ reflection shows a stripe ordering on the (0 1 0) direction. To make compatible this apparent contradicting result, we have two possibilities: (*i*) We can hypothesize that the even-Mn sublattice remains isotropic and anisotropy is only originated from the odd-Mn sublattice. In such a case, the four odd-Mn atoms in the asymmetric cell cannot be identical and differences among them arise either from their anisotropy orientation or from the components of the scattering tensor. (ii) The other possibility implies that the d-projected density of states of the even-Mn

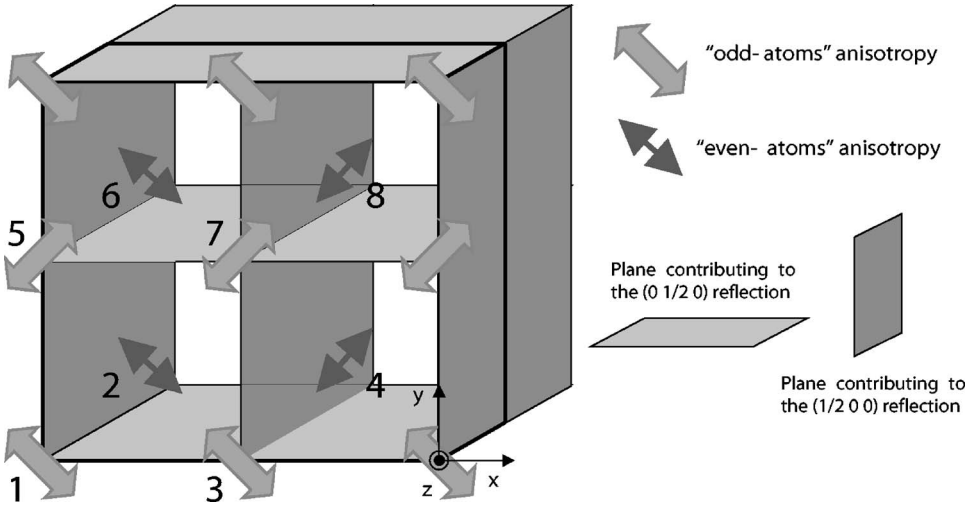

FIG. 8. Schematic view of the double-stripe model in the ab plane. Horizontal and vertical stripes of "odd" and "even" Mn atoms are shown.

atoms is not isotropic. In this case, the even-Mn sublattice can be ordered with a different orientation than the odd-Mn sublattice giving rise to a double stripe formation. In this situation, the odd-Mn sublattice gives a stripe on the (0 1 0) direction and the even-Mn sublattice a (1 0 0) stripe. Although we cannot discard either of these two possibilities, we propose the last one as the most convincing. There are several arguments which support this choice:

(i) The simplicity, only two lattices crystallographically decoupled are necessary to describe this phenomenon.

(ii) The energy dependences of these two resonances are completely different. Some coincidences would be observed in the energy dependence if the resonances originated from the same sublattice.

(iii) The hyphothesis that the even-Mn sublattice is isotropic is not very well supported since the ionic approximation is no longer valid, i.e., the valence is about 3.6+.

According to these arguments, the experimental data are consistent with a double stripe structure. The odd-Mn atoms show an ordering of the local *d* anisotropy following the (1 0 0) direction whereas the *d*-projected states ("*d* orbitals") from the even-Mn sublattice order in the perpendicular direction. Figure 8 shows a pictorial representation of this double ordering. We note that the local *d* anisotropy from the even-Mn sublattice is not accompanied by a structural distortion as for the odd-Mn sublattice. This fact agrees with the lack of observation of $(h/2,0,0)$ reflections at the Mn *K* edge.

As a last point, we discuss the possible correlation between the magnetic and the so-called OO scattering in $Nd_{0.5}Sr_{0.5}MnO_3$. Recently, a detailed theoretical study has addressed an influence of the spin configuration on the orbital scattering spectrum for the low temperature phase of $La_{0.5}Sr_{1.5}MnO_4$.[36] In our case, from the comparison between $(0\ \frac{1}{2}\ 0)$ resonant spectrum and the $(\frac{1}{4}\ \frac{1}{4}\ 0)$ one from $LaSr_2Mn_2O_7$ (Fig. 3), where no magnetic contribution is expected, the strong similarity in both spectra indicates that no contribution from the magnetic scattering should be present in this anisotropic reflection.

V. CONCLUSIONS

We have measured the $(0\ \frac{1}{2}\ 0)$ and $(\frac{1}{2}\ 0\ 0)$ reflections in the low temperature phase of $Nd_{0.5}Sr_{0.5}MnO_3$ by means of RXS at the Mn $L_{2,3}$ edges. Within the checkerboard pattern and following a simple ionic model, the former reflection has been commonly assigned to the orbital ordering of the e_g electrons at the Mn^{3+} ions occupying the tetragonal distorted octahedral sites (odd-Mn). Nevertheless, we have recently shown[18] that ionic CO is a very rough approximation to the real electronic state of Mn in half-doped manganites, the charge separation being much less than 1 e^-. Moreover, the main factor that causes the appearance of the so-called OO reflections at the Mn *K* edge[34,37] is the local anisotropy of the tetragonal distorted Mn sites. The azimuthal evolution of the $(0\ \frac{1}{2}\ 0)$ reflection at the Mn $L_{2,3}$ edges coincides with the behavior of the equivalent $(0\ \frac{5}{2}\ 0)$ reflection at the Mn *K* edge. Therefore, the same tensorial model based on the local distortion satisfactorily explains both results.

The resonant $(\frac{1}{2}\ 0\ 0)$ reflection can be related to the ordering of the even-Mn sublattice (the so-called Mn^{4+}), which is perpendicular to the odd-Mn (so-called Mn^{3+}) sublattice. It presents an azimuthal evolution very much like the one observed in the $(0\ \frac{1}{2}\ 0)$ reflection, with a π periodicity and similar minima (nearly null) and maxima angular positions. Finally, the evolution of the resonant intensity of both reflections as a function of temperature shows that this double ordering appears almost simultaneously at T_N.

So far, resonant scattering at the Mn $L_{2,3}$ edges in half-doped manganites has been explained in the framework of the ionic model, in such a way that observation of a resonant reflection is considered as a direct proof of atomic *d*-orbital ordering. It is worth remarking that this approach is very difficult to be reconciled with the experimental facts. First, RXS experiments at the Mn *K* edge show very small charge segregation between the two inequivalent Mn atoms. Second, the present results from $L_{2,3}$ RXS study show that (*i*) the resonant spectrum of the $(0\ \frac{1}{2}\ 0)$ reflection extends in a broad energy range, near the whole width of the absorption spectra. In the multiplet atomic approach, this would mean that several *d* states are anisotropic, not exclusively the supposed "e_g" ordered orbital. There are two main peaks in the spectra, which would be ascribed to two different *d* orbitals. (*ii*) The features at the $(\frac{1}{2}\ 0\ 0)$ reflection do not seem to be correlated with those observed at the $(0\ \frac{1}{2}\ 0)$ reflection. Then, a new order of the so-called Mn^{4+} atoms seems to occur. (*iii*) The

high similitude between our results and those obtained in $LaSr_2Mn_2O_7$ with a different magnetic ordering seems to point out that the observed anisotropy of the d-symmetry projected empty states does not depend on the type of magnetic ordering.

Summarizing, this experimental study shows that the so-called CO and OO phase of $Nd_{0.5}Sr_{0.5}MnO_3$ is characterized by a double stripe ordering of the two sublattices. Consequently, the unit cell of the orbital ordered structure is now $2a \times 2b \times c$ of the *Ibmm* high temperature space group. On one hand, the OO of the odd-Mn sublattice is accompanied by the local tetragonal distortion. On the other hand, the OO of the even-Mn sublattice is perpendicular to the former and this anisotropy seems to have an intrinsic electronic origin, i.e., a genuine OO without structural coupling.

ACKNOWLEDGMENTS

We are thankful for the financial support from the Spanish CICyT Project No. MAT2005-04562 and from D.G.A. We also acknowledge ESRF and ID08 beamline for granting beam time.

[1] R. M. Kusters, J. Singleton, D. A. Keen, R. Mc Greevy, and W. Hayes, Physica B **155**, 362 (1989).
[2] J. M. D. Coey, M. Viret, and S. Molnar, Adv. Phys. **48**, 167 (1999).
[3] E. Dagotto, T. Hotta, and A. Moreo, Phys. Rep. **344**, 1 (2001).
[4] S.-W. Cheong and H. Y. Hwang, in *Contribution to Colossal Magnetoresistence Oxides*, Monographs in Condensed Matter Science, edited by Y. Tokura (Gordon & Breach, London).
[5] Y. Tomioka, A. Asamitsu, H. Kuwahara, Y. Moritomo, and Y. Tokura, Phys. Rev. B **53**, R1689 (1996).
[6] H. Kuwahara, Y. Tomioka, A. Asamitsu, Y. Moritomo, and Y. Tokura, Science **270**, 961 (1995).
[7] P. G. Radaelli, D. E. Cox, M. Marezio, S.-W. Cheong, P. E. Schiffer, and A. P. Ramirez, Phys. Rev. Lett. **75**, 4488 (1995).
[8] P. G. Radaelli, D. E. Cox, M. Marezio, and S.-W. Cheong, Phys. Rev. B **55**, 3015 (1997).
[9] B. J. Sternlieb, J. P. Hill, U. C. Wildgruber, G. M. Luke, B. Nachumi, Y. Moritomo, and Y. Tokura, Phys. Rev. Lett. **76**, 2169 (1996).
[10] Y. Moritomo, Y. Tomioka, A. Asamitsu, Y. Tokura, and Y. Matsui, Phys. Rev. B **51**, 3297 (1995).
[11] *Resonant Anomalous X-ray Scattering*, edited by G. Materlik, C. J. Sparks, and K. Fisher (North-Holland, Amsterdam, 1991).
[12] J. B. Goodenough, Phys. Rev. **100**, 564 (1955).
[13] Y. Murakami, H. Kawada, H. Kawata, M. Tanaka, T. Arima, Y. Moritomo, and Y. Tokura, Phys. Rev. Lett. **80**, 1932 (1998).
[14] M. v. Zimmerman, J. P. Hill, D. Gibbs, M. Blume, D. Casa, B. Keimer, Y. Murakami, Y. Tomioka, and Y. Tokura, Phys. Rev. Lett. **83**, 4872 (1999).
[15] M. v. Zimmerman, C. S. Nelson, J. P. Hill, D. Gibbs, M. Blume, D. Casa, B. Keimer, Y. Murakami, C. C. Kao, C. Venkataraman, T. Gog, Y. Tomioka, and Y. Tokura, Phys. Rev. B **64**, 195133 (2001).
[16] K. Nakamura, T. Arima, A. Nakazawa, Y. Wakabayashi, and Y. Murakami, Phys. Rev. B **60**, 2425 (1999).
[17] S. B. Wilkins, P. D. Spencer, T. A. W. Beale, P. D. Hatton, M. v. Zimmermann, S. D. Brown, D. Prabhakaran, and A. T. Boothroyd, Phys. Rev. B **67**, 205110 (2003).
[18] J. Herrero-Martín, J. García, G. Subías, J. Blasco, and M. C. Sánchez, Phys. Rev. B **70**, 024408 (2004).
[19] K. J. Thomas, J. P. Hill, S. Grenier, Y.-J. Kim, P. Abbamonte, L. Venema, A. Rusydi, Y. Tomioka, Y. Tokura, D. F. McMorrow, G. Sawatzky, and M. van Veenendaal, Phys. Rev. Lett. **92**, 237204 (2004).
[20] S. Grenier, J. P. Hill, D. Gibbs, K. J. Thomas, M. v. Zimmermann, C. S. Nelson, V. Kiryukhin, Y. Tokura, Y. Tomioka, D. Casa, T. Gog, and C. Venkatamaran, Phys. Rev. B **69**, 134419 (2004).
[21] S. B. Wilkins, N. Stojic, T. A. W. Beale, N. Binggeli, C. W. M. Castleton, P. Bencok, D. Prabhakaran, A. T. Boothroyd, P. D. Hatton, and M. Altarelli, Phys. Rev. B **71**, 245102 (2005).
[22] Y. Murakami, J. P. Hill, D. Gibbs, M. Blume, I. Koyama, M. Tanaka, H. Kawata, T. Arima, Y. Tokura, K. Hirota, and Y. Endoh, Phys. Rev. Lett. **81**, 582 (1998).
[23] T. Mizokawa and A. Fujimori, Phys. Rev. B **56**, R493 (1997).
[24] M. Benfatto, Y. Joly, and C. R. Natoli, Phys. Rev. Lett. **83**, 636 (1999).
[25] C. W. M. Castleton and M. Altarelli, Phys. Rev. B **62**, 1033 (2000).
[26] S. B. Wilkins, P. D. Spencer, P. D. Hatton, S. P. Collins, M. D. Roper, D. Prabhakaran, and A. T. Boothroyd, Phys. Rev. Lett. **91**, 167205 (2003).
[27] S. S. Dhesi, A. Mirone, C. De Nadaï, P. Ohresser, P. Bencok, N. B. Brookes, P. Reutler, A. Revcolevschi, A. Tagliaferri, O. Toulemonde, and G. van der Laan, Phys. Rev. Lett. **92**, 056403 (2004).
[28] U. Staub, V. Scagnoli, A. M. Mulders, K. Katsumata, Z. Honda, H. Grimmer, M. Horisberger, and J. M. Tonnerre, Phys. Rev. B **71**, 214421 (2005).
[29] S. B. Wilkins, P. D. Hatton, M. D. Roper, D. Prabhakaran, and A. T. Boothroyd, Phys. Rev. Lett. **90**, 187201 (2003).
[30] S. B. Wilkins, N. Stojic, T. A. W. Beale, N. Binggeli, P. Bencok, S. Stanescu, J. F. Mitchell, P. Abbamonte, P. D. Hatton, and M. Altarelli, cond-mat/0412435 (unpublished).
[31] R. Kajimoto, H. Yoshizawa, H. Kawano, H. Kuwahara, Y. Tokura, K. Ohoyama, and M. Ohashi, Phys. Rev. B **60**, 9506 (1999); J. Geck, D. Bruns, C. Hess, R. Klingeler, P. Reutler, M. v. Zimmermann, S.-W. Cheong, and B. Büchner, *ibid.* **66**, 184407 (2002).
[32] V. E. Dmitrienko, Acta Crystallogr., Sect. A: Found. Crystallogr. **A39**, 29 (1983).
[33] V. E. Dmitrienko, K. Ishida, A. Kirfel, and E. N. Ovchinnikova, Acta Crystallogr., Sect. A: Found. Crystallogr. **A61**, 481 (2005).
[34] J. García, M. C. Sánchez, J. Blasco, G. Subías, and M. G. Proietti, J. Phys.: Condens. Matter **13**, 3243 (2001).
[35] J. P. Hannon, G. T. Trammell, M. Blume, and D. Gibbs, Phys. Rev. Lett. **61**, 1245 (1988); J. P. Hill and D. F. McMorrow, Acta Crystallogr., Sect. A: Found. Crystallogr. **A52**, 236 (1996).
[36] N. Stojic, N. Binggeli, and M. Altarelli, Phys. Rev. B **72**, 104108 (2005).
[37] J. García and G. Subías, Phys. Rev. B **68**, 127101 (2003).